Biogeosciences, 19, 4351–4360, 2022
https://doi.org/10.5194/bg-19-4351-2022

Biogeosciences Open Access EGU

Rapidly increasing sulfate concentration: a hidden promoter of eutrophication in shallow lakes

Chuanqiao Zhou[1,★], Yu Peng[1,★], Li Chen[1], Miaotong Yu[1], Muchun Zhou[2], Runze Xu[1], Lanqing Zhang[1], Siyuan Zhang[3], Xiaoguang Xu[1], Limin Zhang[1], and Guoxiang Wang[1]

[1]Jiangsu Key Laboratory of Environmental Change and Ecological Construction, Jiangsu Center for Collaborative Innovation in Geographical Information Resource Development and Application, School of Environment, Nanjing Normal University, Nanjing 210023, China
[2]China Aerospace Science and Industry Nanjing Chenguang Group, Nanjing 210022, China
[3]School of Energy and Environment, Southeast University, Nanjing 210096, China
★These authors contributed equally to this work.

Correspondence: Xiaoguang Xu (xxg05504118@163.com)

Received: 21 March 2022 – Discussion started: 4 April 2022
Revised: 18 August 2022 – Accepted: 20 August 2022 – Published: 14 September 2022

Abstract. Except for excessive nutrient input and climate warming, the rapidly rising SO_4^{2-} concentration is considered as a crucial contributor to the eutrophication in shallow lakes; however, the driving process and mechanism are still far from clear. In this study, we constructed a series of microcosms with initial SO_4^{2-} concentrations of 0, 30, 60, 90, 120, and 150 mg L^{-1} to simulate the rapid SO_4^{2-} increase in Lake Taihu, China, subjected to cyanobacteria blooms. Results showed that the sulfate reduction rate was stimulated by the increase in initial SO_4^{2-} concentrations and cyanobacteria-derived organic matter, with the maximal sulfate reduction rate of 39.68 mg $(L\,d)^{-1}$ in the treatment of 150 mg L^{-1} SO_4^{2-} concentration. During the sulfate reduction, the produced maximal $\sum S^{2-}$ concentration in the overlying water and acid volatile sulfate (AVS) in the sediments were 3.15 mg L^{-1} and 11.11 mg kg^{-1}, respectively, and both of them were positively correlated with initial SO_4^{2-} concentrations ($R^2 = 0.97$; R^2 =0.92). The increasing abundance of sulfate reduction bacteria (SRB) was also linearly correlated with initial SO_4^{2-} concentrations ($R^2 = 0.96$), ranging from 6.65×10^7 to 1.97×10^8 copies g^{-1}. However, the Fe^{2+} concentrations displayed a negative correlation with initial SO_4^{2-} concentrations, and the final Fe^{2+} concentrations were 9.68, 7.07, 6.5, 5.57, 4.42, and 3.46 mg L^{-1}, respectively. As a result, the released total phosphorus (TP) in the overlying water, to promote the eutrophication, was up to 1.4 mg L^{-1} in the treatment of 150 mg L^{-1} SO_4^{2-} concentration. Therefore, it is necessary to consider the effect of rapidly increasing SO_4^{2-} concentrations on the release of endogenous phosphorus and the eutrophication in lakes.

1 Introduction

Nowadays, cyanobacteria blooms in eutrophic lakes have become one of the most serious problems in freshwater lakes all over the world (Iwayama et al., 2017; Ho et al., 2019). Phosphorus, as a necessary nutrient for biological growth, is considered to be one of the main limiting factors of lake eutrophication (Ni et al., 2020). In recent years, the input of exogenous phosphorus has been effectively controlled, while the release of endogenous phosphorus is still an urgent problem in eutrophic lakes (Liu et al., 2018; Guo et al., 2020). The release of endogenous phosphorus is affected by many factors, such as wind and waves and the cyanobacteria decomposition (Xu et al., 2018; Zhao et al., 2019). There are many forms of phosphorus in freshwater lake sediments, including aluminum bound phosphorus (Al-P), iron bound phosphorus (Fe-P), etc. Among them, Fe-P, formed under the condition of high dissolved oxygen (DO), is the most active form of phosphorus in the sediments, which has a more obvious response to the change in DO (Zhang et al., 2020). The accumulation and decay of cyanobacteria in eutrophic lakes will change the physical and chemical environments of the wa-

ter body and form anaerobic reduction conditions (Yan et al., 2017). This will facilitate the reduction of iron oxides and lead to the desorption and release of Fe-P in sediments, resulting in the increase in endogenous phosphorus release (Zhao et al., 2019).

Iron reduction plays an important role in natural ecosystems. It has been reported that dissimilatory reduction of iron accounts for 22 % of the total amount of organic matter anaerobic mineralization in offshore areas (Thamdrup et al., 2004). According to the classical theory, iron oxides or hydroxides can adsorb phosphorus in the water and form Fe-P precipitation (Gunnars and Blomqvist, 1997). In freshwater lakes, the lack of Fe(III) content or the diagenesis of organic phosphorus may be the reason for the lack of phosphorus in the overlying water. Therefore, the formation of iron oxides on the surface of sediments is closely related to the phosphorus cycle process (Amirbahman et al., 2003; Chen et al., 2014). The interaction between iron and phosphorus is reflected in the effect of adsorption and desorption of Fe oxide on the phosphorus content in the overlying water, since Fe-P is the main internal source of phosphorus (Wu et al., 2019). Iron oxides can be used as both the source and destination of phosphorus in lake ecosystems (Mort et al., 2010; Azam and Finneran, 2014). In anaerobic reduction environments, iron reduction can significantly promote the resolution of Fe-P. The Fe^{2+} generated by the reaction can form solid FeS with soluble sulfide. In addition, free Fe^{3+} will combine with humus to form a stable complex, which further prevents the co-precipitation process of phosphorus and iron oxides (Mort et al., 2010; Zhang et al., 2020). Therefore, the iron reduction process driven by cyanobacteria decomposition affects the circulation of phosphorus in freshwater lakes.

Due to the SO_4^{2-} concentration in seawater reaching 28 mM, the sulfate reduction process with the participation of sulfate reduction bacteria (SRB) has received considerable attention in the basic material cycle of marine biogeochemistry (Fike et al., 2015; Pan et al., 2020). In freshwater lakes, the SO_4^{2-} concentration is less than 800 µM, which is generally considered insufficient for continuous sulfate reduction (Hansel et al., 2015). However, in recent years, with the continuous input of exogenous sulfur, the SO_4^{2-} concentration in freshwater lakes increases significantly, and the degree of the eutrophication and the SO_4^{2-} concentration show a positive correlation (Dierberg et al., 2011; Yu et al., 2013). For instance, the SO_4^{2-} concentration in Lake Taihu, China, one of the typical eutrophic lakes, has increased from 30 to 100 mg L^{-1} in the past 70 years, and it will continue to rise in the future (Yu et al., 2013; Zhou et al., 2022). The impact of sulfate reduction on the material cycle of lake ecosystems may be far beyond our knowledge (Baldwin and Mitchell, 2012; Yu et al., 2013). On the other hand, it has been reported that the sulfate reduction process is one of the important ways of anaerobic metabolism of organic matter in freshwater lakes, and $\sum S^{2-}$ produced by the sulfate reduction process can mediate the iron reduction process (Jorgensen et al., 2019; Zhang et al., 2020). SRB mainly use SO_4^{2-} as the electron acceptor to complete anaerobic respiration, and the sulfur compounds produced by anaerobic metabolism are bound with iron and so on, which are fixed in the sediments and form AVS on the surface of sediments (Holmer and Storkholm, 2001; Chen et al., 2016). Therefore, with the input of exogenous sulfur, $\sum S^{2-}$ produced through the sulfate reduction process will further promote iron reduction in freshwater lakes.

In freshwater lakes, the iron cycle affects the process of the phosphorus cycle, and the sulfur cycle plays an important role in regulating the iron cycle. Therefore, the cycle of iron, sulfur, and phosphorus in freshwater lakes is inseparable (Wu et al., 2019; Zhao et al., 2019). Studies have shown that even when SO_4^{2-} content was as low as 20 mg L^{-1}, the anaerobic metabolism of organic substrates was still dominated by sulfate reduction. Therefore, the sulfate reduction process plays an important role in the lacustrine biochemical cycle (Hansel et al., 2015). In the absence of cyanobacteria, sulfate reduction does not occur even if the SO_4^{2-} concentration is higher (Zhao et al., 2021). This is because the accumulation and decomposition of cyanobacteria not only change the environment of the water body but also release a large amount of organic matter, which provides the necessary conditions for the circulation of iron, sulfur, and phosphorus (Yan et al., 2017; Melemdez-Pastor et al., 2019). Therefore, under the co-effect of the increase in SO_4^{2-} and the cyanobacteria decomposition, the sulfate reduction process and the effect of the iron reduction process on endogenous phosphorus release from sediments need to be further studied.

In this study, a series of different initial concentrations of SO_4^{2-} were set according to the variation trend of SO_4^{2-} concentrations over the years and the possible rising trend in the eutrophic Lake Taihu. The effects of increased SO_4^{2-} concentration and cyanobacteria bloom on sulfate reduction coupled with the microbial processes were investigated. The dynamic changes in Fe^{2+} and Fe^{3+} concentrations during iron reduction were studied in order to reveal the effect of sulfate reduction on iron reduction. In addition, the dynamic changes in phosphorus in the overlying water and sediment were investigated. Finally, the coupled sulfate, iron, and phosphorus cyclic processes affected by the increasing sulfate concentration and cyanobacteria bloom were also comprehensively analyzed for elucidating the phosphorus release dynamics to tracking the hidden promoter of cyanobacteria blooms in eutrophic lakes. The findings may be beneficial for evaluating the effect of sulfate reduction in freshwater lakes and its impact on the promotion of iron reduction and the release of endogenous phosphorus.

2 Materials and methods

2.1 Sample collection and preparation

Lake Taihu (31°24′40″ N, 120°1′3″ E) is one of the largest eutrophic shallow lakes in China, with an average depth of 2.4 m and an area of 2340 m^2 (Mao et al., 2021). In this study, samples of sediments and cyanobacteria were collected in July 2020. Sediments (0–20 cm) from the west shoreline of the lake (31°24′45″ N, 120°0′42″ E) were collected using a gravity core sampler (length of 150 cm and diameter of 20 cm). Cyanobacteria was collected and concentrated by sieving water through a fine-mesh plankton (250 mesh). All the sediment and cyanobacteria samples were stored in an incubator with ice packs and delivered to the laboratory immediately. The sediment samples were blended thoroughly, homogenized, and sieved (100 mesh) to the polyethylene bag. The cyanobacteria samples were flushed and centrifuged at 1500 rpm for 5 min by a CT15RT versatile refrigerated centrifuge (China) and freezed dried by Biosafer-10A. Different gradient sulfate concentrations were prepared from the high-purity water and Na_2SO_4.

2.2 Setup of incubation microcosms

To simulate the dramatic SO_4^{2-} increase and cyanobacteria blooms of eutrophic Lake Taihu, a series of microcosms were constructed in this study. According to the ratio of surface sediments and the average water depth and the cyanobacteria accumulation density of 2500 g m^{-2} during the breakout of cyanobacteria blooms of Taihu Lake, 100 g of sediment, 200 mL of water, and 0.11 g of cyanobacteria powder were added into each bottle (Zhang et al., 2020). Meanwhile, according to the change trend of SO_4^{2-} concentrations in Taihu Lake over the years and the possibility of further increase in the future (Yu et al., 2013), the SO_4^{2-} concentrations in six microcosm systems were configured as 30, 60, 90, 120, and 150 mg L^{-1}, as well as a control without SO_4^{2-}. The microcosm system adopted anaerobic bottles (Φ75 mm, length 180 mm, volume 500 mL) as the reaction device. There were three replicates in each SO_4^{2-} concentration experimental group. Each group was sampled 17 times after 1, 2, 3, 4, 5, 6, 7, 9, 11, 14, 18, 23, 28, 33, 38, 43, and 48 d. Totally, there were 306 anaerobic bottles, and all the anaerobic bottles were placed in a biochemical incubator at a temperature of 25°C. The water, gas, and soil samples were collected by destructive sampling; that is, at each sampling point, 18 anaerobic bottles were opened for testing, which ensured the anaerobic environment and air pressure for other bottles. A part of sediment was used for microbe determination and kept in a refrigerator at −80°C, and the rest of the sediment and other samples were kept at 0–4°C for less than 24 h before analysis.

2.3 Chemical analytical methods

All water samples were filtered through 0.45 µm Nylon filters. Dissolved total phosphorus (DTP) was determined by colorimetry after digestion with $K_2S_2O_8 + NaOH$, and the ammonium molybdate and ascorbic acid were used as chromogenic agents (Ebina et al., 1983). Water DO and oxidation and reduction potential were measured using calibrated probes (MP525, China) during destructive sampling. The SO_4^{2-} was detected using the turbidimetric method with the stabilizer of $BaCl_2$ and gelatin (Tabatabai, 1974), and the $\sum S^{2-}$ was detected by methylene blue (Cline et al., 1969). Fe^{2+} and Fe^{3+} were determined by colorimetric analysis (Phillips and Lovely, 1987). The sediment total phosphorus (TP) was extracted and determined by colorimetry (Ruban et al., 2001). The schematic diagram of the method to test acid volatile sulfate (AVS) is shown in Fig. S5 in the Supplement; briefly, 5 g of sediment was put into a 250 mL glass flask, and inside a small beaker with 15 mL of $ZnAc_2 \cdot 2H_2O$ and $NaAc \cdot 3H_2O$ was used to absorb H_2S gas. The tube A was connected by N_2 for 5 min in order to discharge the air in the bottle from pipe B, and then the valves of tubes A and B were closed. A total of 2 mL ascorbic acid solution was added to prevent S^{2-} oxidation, and then 15 mL (6 mol L^{-1}) of hydrochloric acid was added with the reaction at room temperature for 18 h. AVS was determined by the zinc cold diffusion method (Hsieh and Shieh, 1997).

2.4 Quantification of SRB in sediments

In order to confirm the changes in sediment SRB in the microcosms, quantitative reverse transcription polymerase chain reaction (RT-qPCR) technologies were used to determine the cell copy numbers of methane-producing archaea (MPA) and SRB after 0.7 and 38 d in the sediments.

The sediment samples were collected and frozen at −80°C in an ultra-low-temperature freezer. The E.Z.N.A.® Soil DNA Kit (Omega Bio-Tek, Norcross, GA, USA) was used to extract the total genomic DNA from each soil sample according to the manufacturer's instructions. Nucleic acid quality and concentration were determined by 1 % agarose gel electrophoresis and NanoDrop 2000 UV spectrophotometer (Thermo Scientific, USA), respectively.

SRB in sediments were quantified using the quantitative polymerase chain reaction (qPCR) method. The qPCR with primer sets targeting DSR1F+ (5′-ACSCACTGGAAGCACGGCGG-3′) and DSR-R (5′-GTGGMRCCGTGCAKRTTGG-3′) was used for the SRB in this study. The qPCR experiments were performed on a ABI7300 qPCR instrument (Applied Biosystems, USA) using ChamQ SYBR Color qPCR Master Mix as the signal dye. Each 20 µL reaction mixture contained 2 µL of the template DNA and 16.5 µL of ChamQ SYBR Color qPCR Master Mix. Standard curves for each gene were obtained by the 10-fold serial dilution of standard plasmids containing

the target functional gene. All operations followed the Minimum Information for Publication of Quantitative Real-Time PCR Experiments (MIQE) guidelines.

2.5 Statistical analysis

The Statistical Package of the Social Science 18.0 (SPSS 18.0) was used for statistical analysis. The one-way analysis of variance (ANOVA) and correlation analysis were carried out using bivariate correlations analysis.

3 Results

3.1 Fe^{2+} and Fe^{3+} dynamics in overlying water

The concentration variations of Fe^{2+} and Fe^{3+} in overlying water during the incubation are presented in Fig. 1. In the treatment without SO_4^{2-}, they increased continuously to 9.68 and 10.15 mg L^{-1}, respectively. The concentration of Fe^{3+} in the remaining five treatments decreased at the beginning and then increased to keep stable. The higher the initial sulfate concentration was, the lower the final Fe^{3+} concentration was. In the initial 150 mg L^{-1} SO_4^{2-} concentration treatment, the final Fe^{3+} concentration was the lowest at 7.7 mg L^{-1}. The Fe^{2+} concentration in the five treatments supplemented with SO_4^{2-} decreased significantly from 11 to 23 d and then increased to a stable level. The final concentration of Fe^{2+} also showed a negative correlation with the initial concentration of SO_4^{2-}. In the initial 30 mg L^{-1} SO_4^{2-} concentration treatment, the final Fe^{2+} concentration was the highest at 7.07 mg L^{-1}.

3.2 SO_4^{2-} and $\sum S^{2-}$ dynamics in overlying water

All treatments had an obvious sulfate reduction reaction, and the concentration of SO_4^{2-} decreased greatly except for the treatment without adding SO_4^{2-} (Fig. 2). The higher the initial sulfate concentration was, the faster the sulfate reduction rate in the initial stage was (Table 1). In the treatment with initial SO_4^{2-} concentration of 150 mg L^{-1}, the sulfate reduction rate was 39.68 mg $(L\,d)^{-1}$, while it was only 9.39 mg $(L\,d)^{-1}$ in the 30 mg L^{-1} SO_4^{2-} treatment. The sulfate reduction rate at the beginning of other treatments was also positively correlated with the initial SO_4^{2-} concentration.

The higher the initial SO_4^{2-} concentration was, the higher the maximum concentration of $\sum S^{2-}$ was. In the treatment with initial SO_4^{2-} concentration of 30 mg L^{-1}, the lowest concentration was 2.93 mg L^{-1} on the fifth day. However, the lowest SO_4^{2-} concentration appearing on the 23rd day was 1.18 mg L^{-1} in the treatment with the initial SO_4^{2-} concentration of 150 mg L^{-1}. The maximum concentration of $\sum S^{2-}$ was positively correlated with the initial SO_4^{2-} concentration. In the initial SO_4^{2-} concentrations of 30, 60, 90, 120, and 150 mg L^{-1} SO_4^{2-} treatments, the highest $\sum S^{2-}$ concentrations at 7 d were 0.61, 1.14, 1.55, 2.15, and 3.15 mg L^{-1}, respectively.

Table 1. Sulfate reduction rate in the water column of microcosms (mg $(L\,d)^{-1}$).

SO_4^{2-}	Time (d)		
(mg L^{-1})	0	7	38
0	–	–	–
30	9.39	0.74	0.05
60	9.44	2.84	0.07
90	28.02	4.98	0.11
120	30.89	19.45	0.11
150	39.68	10.42	0.21

3.3 TP dynamics in overlying water and sediments

The dynamics of DTP concentrations in overlying water during the incubation are presented (Fig. 3a). The concentrations of DTP in overlying water were positively correlated with the initial SO_4^{2-}. The higher the initial concentrations of SO_4^{2-} were, the higher the concentrations of DTP in overlying water were. On day 11, DTP in overlying water continued to rise and then kept stable. The highest DTP concentration was 2.08 mg L^{-1} in the treatment with the initial SO_4^{2-} concentration of 150 mg L^{-1}, while the highest DTP concentration was 0.36 mg L^{-1} in the treatment without SO_4^{2-} addition.

The concentrations of TP in the sediments increased significantly in all treatments with the cyanobacteria decomposition in the initial stage (Fig. 3b). Among all treatments, on the ninth day, the highest concentration of TP in the sediments was 887.69 mg kg^{-1} in the treatment with the initial SO_4^{2-} concentration of 0 mg L^{-1}. After 23 d, TP in the sediments decreased significantly and then stabilized. During cyanobacteria decomposition and sulfate reduction, the concentrations of TP in all treatments negatively correlated with the initial SO_4^{2-} concentration. The final TP concentrations were 448.92, 335.32, 321.56, 259.32, 238.56, and 227.21 mg kg^{-1} in all treatments.

3.4 AVS dynamics in the sediments

The concentrations of AVS in the sediments were positively correlated with the initial SO_4^{2-} concentrations. With the increase in TP in overlying water, the AVS in the sediments also increased steadily and reached the peak on the 11th day. In the treatments with the initial SO_4^{2-} concentrations of 0, 30, 60, 90, 120, and 150 mg L^{-1}, the highest concentrations of AVS in the sediments were 7.21, 7.99, 8.54, 8.99, 9.34, and 11.11 mg kg^{-1}, respectively.

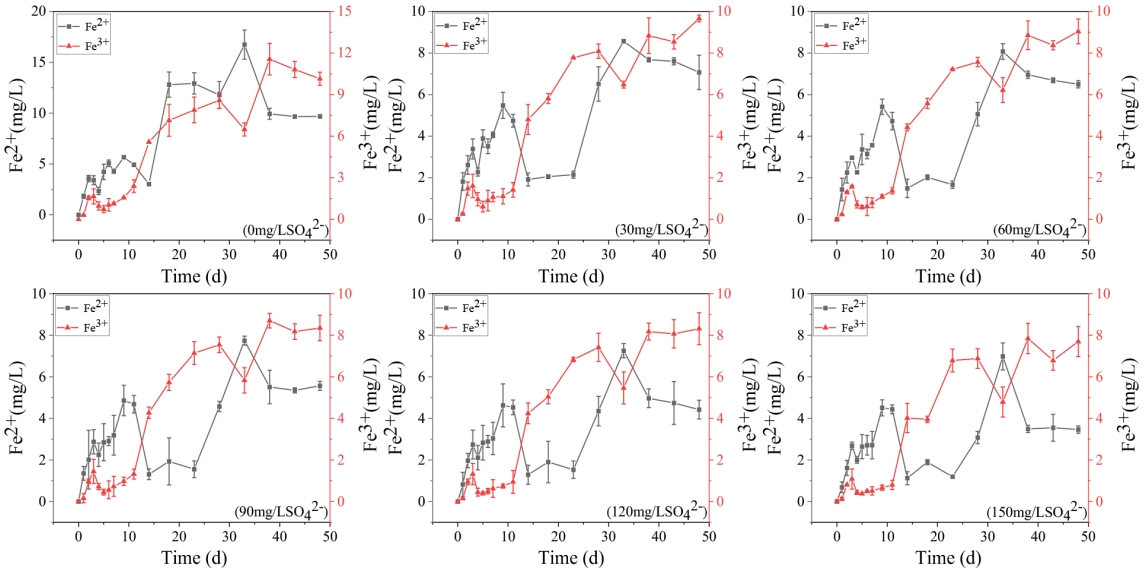

Figure 1. The concentration variations of Fe^{2+} and Fe^{3+} in the water column during the incubation.

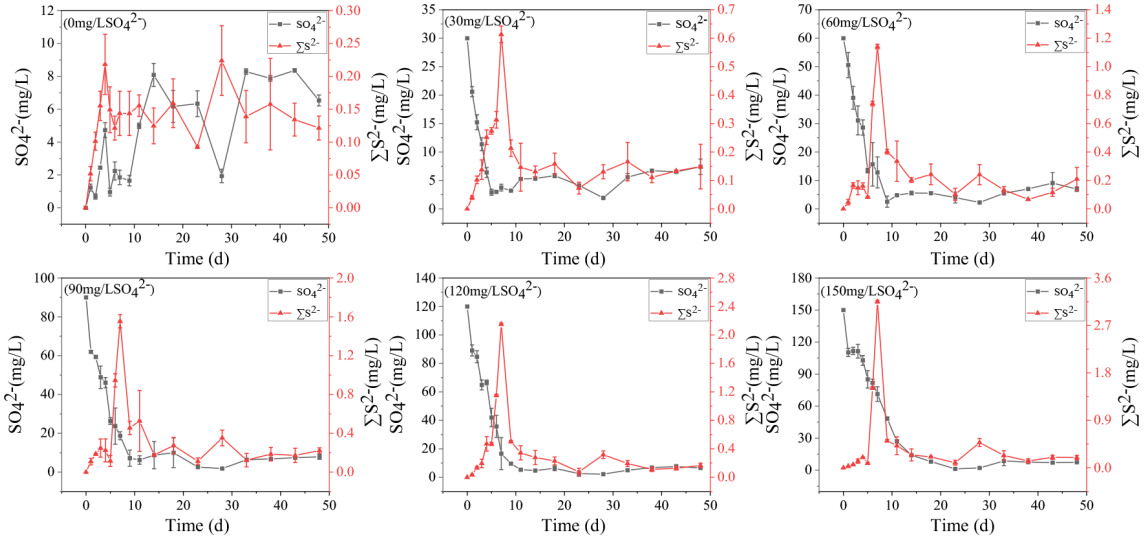

Figure 2. The concentration variations of SO_4^{2-} and $\sum S^{2-}$ in the water column during the incubation.

3.5 SRB dynamics in the sediments

During the decomposition of cyanobacteria, the SRB abundance significantly increased compared with the initial stage ($P < 0.01$). In the initial stage, the SRB abundance was 1.09×10^8 copies g^{-1} and the final value was positively correlated with the initial SO_4^{2-}. On day 7, SRB of all treatments showed a downward trend compared with the initial value, and there was no significant difference in SRB values between each treatment. On day 38, except for the initial SO_4^{2-} concentrations of 0 and 30 mg L^{-1}, SRB increased significantly in other treatments.

4 Discussion

It is generally acknowledged that climate warming and exogenous nutrient input are the important contributors to the occurrence of cyanobacteria blooms (Anneville et al., 2015; Yan et al., 2017). However, in this study, we found that the dramatically increasing SO_4^{2-} concentration in eutrophic lakes is also a non-negligible promoter for the self-sustainment of cyanobacteria blooms. In eutrophic lakes, the decomposition of cyanobacteria consumed DO in the water and formed strong anaerobic reduction conditions (Fig. S1). Fe-P was desorbed to form free Fe^{3+}, which was reduced to Fe^{2+} in anaerobic environments (Fig. 1). Free Fe^{2+} com-

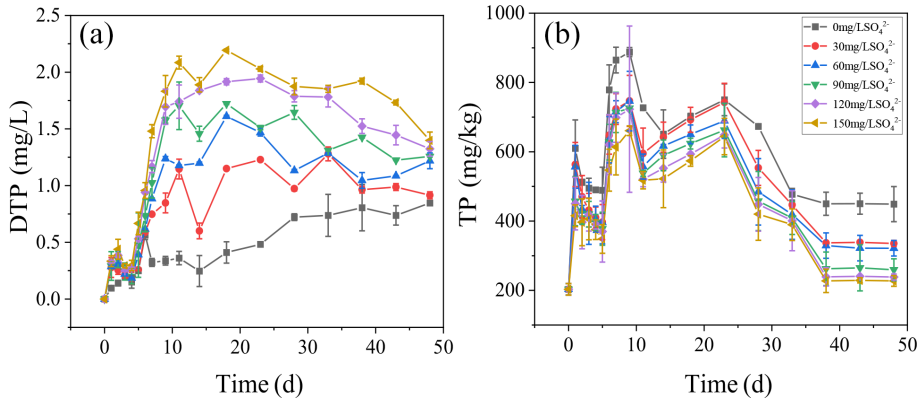

Figure 3. The concentrations of TP in the overlying water **(a)** and sediments **(b)** during the incubation.

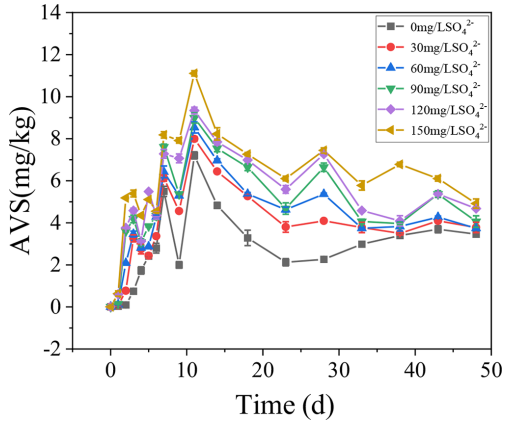

Figure 4. The concentration of AVS in the sediments during the incubation.

Table 2. Copy numbers of the *dsrB* gene of SRB in the sediments during the incubation (copies g^{-1}).

SO_4^{2-}	Time		
($mg\,L^{-1}$)	0 d	7 d	38 d
0	1.09×10^8	5.81×10^7	6.65×10^7
30	1.09×10^8	6.13×10^7	7.71×10^7
60	1.09×10^8	7.61×10^7	1.15×10^8
90	1.09×10^8	7.87×10^7	1.31×10^8
120	1.09×10^8	7.99×10^7	1.49×10^8
150	1.09×10^8	8.23×10^7	1.91×10^8

bined with $\sum S^{2-}$ which was generated by sulfate reduction and eventually formed AVS fixed in the sediments (Fig. 4), and phosphorus was released from the sediments (Fig. 3). It has been reported that SRB and iron reduction bacteria (IRB) are the main microorganisms that drive sulfate reduction and iron reduction, respectively, and cyanobacteria decomposition promotes these microorganisms' growth (Wu et al., 2019). Consistent with these results, our findings also revealed that cyanobacteria released large amounts of organic matter to promote microbial growth during their decay and decomposition (Fig. S2, Table 2) and ultimately promoted anaerobic reduction of sulfur and iron (Holmer et al., 2001). Therefore, with increasing SO_4^{2-} concentrations in eutrophic lakes, the influence of sulfate reduction on phosphorus release is worth further investigation.

The iron, sulfur, and phosphorus cycles are inseparable in lake sediments (Zhang et al., 2020). With the increase in SO_4^{2-} concentration in eutrophic lakes, the effect of sulfate reduction on phosphorus release from sediments may be more important than previously recognized (Pester et al., 2012). Sulfate reduction driven by SRB is an important organic metabolism pathway in natural systems. During the sulfate reduction process, SO_4^{2-} is an electron acceptor, and its concentration variation can significantly affect the sulfate reduction rate (Holmer and Storkholm, 2001; Nakagawa et al., 2012). SO_4^{2-} is reduced to $\sum S^{2-}$ by acquiring the electrons supplied by SRB oxidation, and thus SRB play an important role in sulfate reduction (Sela-Adler et al., 2017). The increase in SO_4^{2-} concentration promotes the SRB abundance, as evidenced by a positive correlation (Wu et al., 2019). In the case of increased SRB abundance (Table 2) and increased SO_4^{2-} concentration, the sulfate reduction reaction was enhanced. The SO_4^{2-} concentration in the overlying water decreased significantly accompanied by a temporary increase in $\sum S^{2-}$ (Fig. 2). The highest concentrations of $\sum S^{2-}$ also increased with the initial SO_4^{2-} concentrations (Fig. 5a). Interestingly, the $\sum S^{2-}$ decreased rapidly after day 10 to almost zero at the end (Fig. 2). This may result from two key factors: (a) hydrogen sulfide overflows from the incubator, and s (b) sulfide migrates downward and combines with other substances in the sediment and is immobilized (Zhang et al., 2020). In this study, TP in the overlying water has a significant positive correlation with the initial SO_4^{2-} concentrations ($R^2 = 0.96$; Fig. 3). The classical theory presumes that iron reduction by IRB leads to the release of iron-

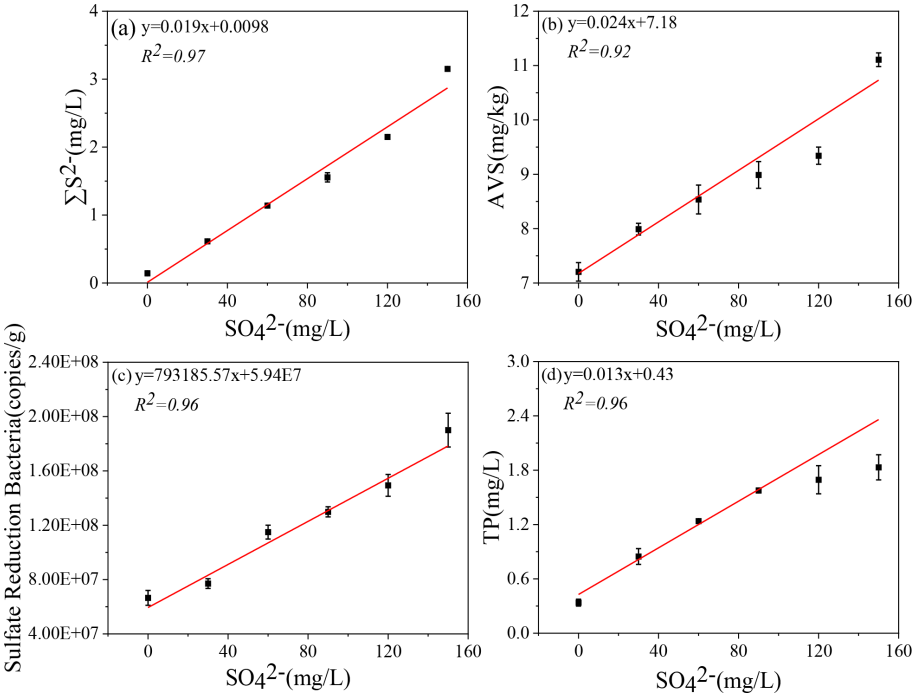

Figure 5. Correlation of initial SO_4^{2-} concentrations with $\sum S^{2-}$ **(a)**, AVS **(b)**, sulfate-reducing bacteria (SRB) **(c)**, and TP **(d)** in the microcosm systems.

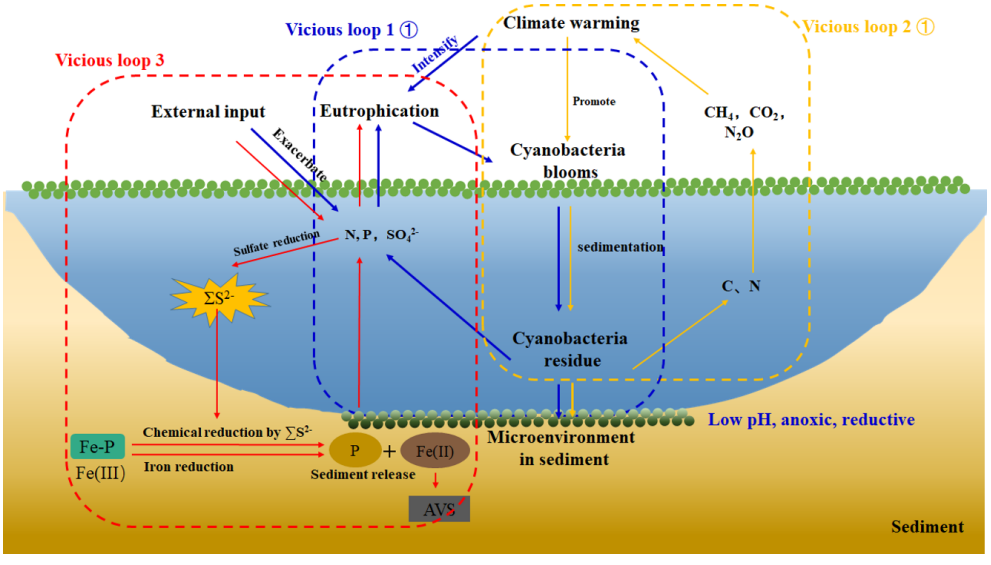

Figure 6. A simplified scheme of the relationship among climate warming, lake eutrophication, and cyanobacteria blooms in eutrophic lakes. Under climate warming scenarios, extreme abiotic and biotic conditions facilitated the breakout of cyanobacteria blooms. After their collapse, the high amount of N, P, and C were released into the overlying water and reacted with the eutrophication. Furthermore, a large amount of CH_4 and CO_2 was produced and emitted to the atmosphere, contributing to global warming from freshwater lakes (Yan et al., 2017). With the external sulfur input, the concentration of SO_4^{2-} increased significantly, and sulfate reduction was enhanced. The cyanobacteria decomposition created an anaerobic reduction environment, which will promote iron reduction and sulfate reduction. The free Fe^{3+} generated by Fe-P desorption was reduced to Fe^{2+} and combined with $\sum S^{2-}$, which through sulfate reduction formed stable Fe-S in the sediments. Phosphorus was released from the sediment into the overlying water. Therefore, there are three vicious loops between cyanobacteria bloom occurrence, lake eutrophication, and climate warming.

bound phosphorus in the anaerobic layer of sediments, and when the formed Fe^{2+} enters the aerobic water layer, it is oxidized by Fe^{3+} and bound to phosphorus again (Roden, 2006; Chen et al., 2016). When the sulfate reduction process mediates the iron reduction process, the released Fe^{2+} combines with the product $\sum S^{2-}$ of sulfate reduction to form Fe-S, thus weakening the reoxidation process of Fe^{2+} and increasing the release of phosphorus (Mort et al., 2010; Zhao et al., 2019). Therefore, with the increase in SO_4^{2-} concentrations in eutrophic lakes, it significantly promoted the release of endogenous phosphorus from the sediments.

From a thermodynamic point of view, iron reduction should take precedence over sulfur reduction (Han et al., 2015). However, due to chemical kinetics, sulfur reduction occurs before iron reduction, resulting in the simultaneous appearance of $\sum S^{2-}$ and iron oxides (Han et al., 2015; Hansel et al., 2015). This is consistent with the concentration variation of iron and sulfur in this study (Figs. 1–3). It has been reported that iron cycles in the water body will produce an intense response to the accumulation of sulfide; that is, sulfate reduction can promote iron reduction (Friedrich and Finster, 2014; Zhang et al., 2020). $\sum S^{2-}$ is the final product of sulfate reduction, which is toxic to microorganisms and easy to combine with heavy metals such as Fe^{2+} to form AVS in lake sediments (Holmer et al., 2001). In this study, the concentration of AVS showed a significant positive correlation with the initial concentration of SO_4^{2-} (Figs. 4, 5b), which was consistent with the highest concentration of $\sum S^{2-}$ observed in the overlying water (Figs. 2, 5c). The concentrations of Fe^{2+} and Fe^{3+} in the overlying water increased significantly, and Fe^{2+} significantly decreased in the middle of the incubation (Fig. 1), suggesting that Fe^{2+} reduced by sulfate can be combined with the product $\sum S^{2-}$ (Fig. 2). These results are consistent with the trend that AVS in the sediments reached a peak after 11 d and $\sum S^{2-}$ in the water decreased rapidly after 9 d and remained at a lower concentration (Figs. 2, 3). The reason for this phenomenon may be the formation of Fe-S compounds that are finally fixed in the sediments (Zhao et al., 2019).

The $\sum S^{2-}$-mediated iron chemical reduction may lead to more environmental effects, such as phosphorus mobilization (Zhang et al., 2020). For instance, a previous investigation on the lakes along the Yangtze River demonstrates that the effects of endogenous phosphorus release is probably related to the increase in SO_4^{2-} concentration (Chen et al., 2016). In this study, the concentration of Fe^{2+} in the treatment without SO_4^{2-} continued to rise and was up to the highest concentration among all treatments (Fig. 1). In contrast, the concentrations of TP in the treatment without SO_4^{2-} showed the lowest concentration among all treatments (Figs. 1, 5a). This is caused by Fe^{2+} and Fe^{3+} recombining with phosphorus and being immobilized in the sediments (Wu et al., 2019). In general, iron combines with phosphorus to form siderite ($FePO_4 \cdot 2H_2O$) and blue iron ($Fe_3(PO_4)_2 \cdot 8H_2O$) and is bound to the sediments (Taylor and Konhauser, 2011). However, when precipitation or reduction separates iron from iron phosphate minerals, phosphorus bound to iron is released (Gu et al., 2016).

In order to further elucidate whether the increasing SO_4^{2-} concentrations in overlying water result in the self-sustainment of eutrophication in shallow lakes, a conceptual diagram was put forward (Fig. 6). It has been accepted that exogenous nutrient inputs and climate warming have positive effects on the breakout of cyanobacteria blooms. With the continuous input of exogenous sulfur, the SO_4^{2-} concentration in the lake water increases significantly. When cyanobacteria blooms start to decay, the overlying water shifts from the aerobic state to the strong anaerobic state, providing a carbon source to promote the growth of microorganisms such as SRB. The increasing SO_4^{2-} concentrations provide the electron for the sulfate reduction process, resulting in the sulfate reduction and the release of a large amount of $\sum S^{2-}$. The Fe^{2+} released from the iron reduction process is captured by $\sum S^{2-}$, and finally the combination of iron and phosphorus was reduced, promoting the release of endogenous phosphorus. Therefore, it is necessary to pay attention to the effect of enhanced sulfate reduction on endogenous phosphorus release in eutrophic lakes.

5 Conclusion

The dramatic increase in SO_4^{2-} concentration was up to more than $100\,mg\,L^{-1}$ in eutrophic lakes. There was a coupling relationship between sulfur, iron, and phosphorus cycles in lake ecosystems. The rapidly increasing sulfate concentration enhanced the sulfate reduction to release a large amount of $\sum S^{2-}$ mediated by the increasing abundance of SRB with the adequate organic source from the decay processes of cyanobacteria blooms. The iron reduction showed a positive relationship with the initial sulfate concentrations during the cyanobacteria decomposition. The Fe^{2+} released from the iron reduction process was captured by $\sum S^{2-}$, and finally the combination of iron and phosphorus was reduced, promoting the release of endogenous phosphorus. Therefore, except for climate warming and excessive nutrients, the increasing sulfate concentration has been proven to be another hidden promoter of eutrophication in shallow lakes.

Data availability. The data used in this paper can be accessed by contacting the first author (chuanqiaozhou@163.com) based on a reasonable request.

Supplement. The supplement related to this article is available online at: https://doi.org/10.5194/bg-19-4351-2022-supplement.

Author contributions. XX designed and led the study. CZ, YP, LC, MY, MZ, RX, LaZ, and SZ performed the investigation and analyzed the samples. CZ and YP wrote the original draft with major edits and inputs from XX, LiZ, and GW.

Competing interests. The contact author has declared that none of the authors has any competing interests.

Disclaimer. Publisher's note: Copernicus Publications remains neutral with regard to jurisdictional claims in published maps and institutional affiliations.

Acknowledgements. We thank the editors and the anonymous referees for their insightful comments which substantially improved this paper.

Financial support. This work was supported by the National Natural Science Foundation of China (grant nos. 42077294, 41877336, 41971043), the Cooperation and Guidance Project of Prospering Inner Mongolia through Science and Technology (grant no. 2021CG0037), the National Key Research and Development Program of China (grant no. 2021YFC3200304), and the Guangxi Key Research and Development Program of China (grant no. 2018AB36010).

Review statement. This paper was edited by Aninda Mazumdar and reviewed by four anonymous referees.

References

Amirbahman, A., Pearce, A. R., Bouchard, R. J., Norton, S. A., and Kahl, J. S.: Relationship between hypolimnetic phosphorus and iron release from eleven lakes in Maine, USA, Biogeochemistry, 65, 369–385, https://doi.org/10.1023/A:1026245914721, 2003.

Anneville, O., Domaizon, I., Kerimoglu, O., Rimet, F., and Jacquet, S.: Blue-Green algae in a "Greenhouse Century"? new insights from field data on climate change impacts on cyanobacteria abundance, Ecosystems, 18, 441–458, https://doi.org/10.1007/s10021-014-9837-6, 2015.

Azam, H. M. and Finneran, K. T.: Fe(III) reduction-mediated phosphate removal as vivianite ($Fe_3(PO_4)_2 \cdot 8H_2O$) in septic system wastewater, Chemosphere, 97, 1–9, https://doi.org/10.1016/j.chemosphere.2013.09.032, 2014.

Baldwin, D. S. and Mitchell, A.: Impact of sulfate pollution on anaerobic biogeochemical cycles in a wetland sediment, Water Res., 46, 965–974, https://doi.org/10.1016/j.watres.2011.11.065, 2012.

Chen, M., Ye, T. R., Krumholz, L. R., and Jiang H. L.: Temperature and cyanobacteria bloom biomass influence phosphorous cycling in eutrophic lake sediments, Plos One, 9, e93130, https://doi.org/10.1371/journal.pone.0093130, 2014.

Chen, M., Li, X. H., He, Y. H., Song, N., Cai, H. Y., Wang, C. H., Li, Y. T., Chu, H. Y., Krumholz, L. R., and Jing, H. L.: Increasing sulfate concentrations result in higher sulfide production and phosphorous mobilization in a shallow eutrophic freshwater lake, Water Res., 96, 94–104, https://doi.org/10.1016/j.watres.2016.03.030, 2016.

Cline, J. D.: Spectrophotometric determination of hydrogen sulfide in natural waters, Limnol. Oceanogr., 14, 454–458, 1969.

Dierberg, F. E., DeBusk, T. A., Larson, N. R., Kharbanda, M. D., Chan, N., and Gabriel, M. C.: Effect of sulfate amendments on mineralization and phosphorus release from South Florida (USA) wetland soils under anaerobic conditions, Soil Biol. Biochem., 43, 31–45, https://doi.org/10.1016/j.soilbio.2010.09.006, 2011.

Ebina, J., Tsutsui, T., and Shirai, T.: Simultaneous determination of total nitrogen and total phosphorus in water using peroxodisulfate oxidation, Water Res., 17, 1721–1726, 1983.

Fike, D. A., Bradley, A. S., and Rose, C. V.: Rethinking the ancient sulfur cycle, Annual Review of Earth and Planetary Science, 43, 593–622, https://doi.org/10.1146/annurev-earth-060313-054802, 2015.

Friedrich, M. W. and Finster, K. W.: How sulfur beats iron, Science, 344, 974–975, https://doi.org/10.1126/science.1255442, 2014.

Gu, S., Qian, Y. G., Jiao, Y., Li, Q. M., Pinay, G., and Gruau, G.: An innovative approach for sequential extraction of phosphorus in sediments: Ferrous iron P as an independent P fraction, Water Res., 103, 352–361, https://doi.org/10.1016/j.watres.2016.07.058, 2016.

Gunnars, A. and Blomqvist, S.: Phosphate exchange across the sediment-water interface when shifting from anoxic to oxic conditions an experimental comparison of freshwater and brackish-marine systems, Biogeochemistry, 37, 203–226, 1997.

Guo, M. L., Li, X. L., Song, C. L., Liu, G. L., and Zhou, Y. Y.: Photo-induced phosphate release during sediment resuspension in shallow lakes: A potential positive feedback mechanism of eutrophication, Environ. Pollut., 258, 113679, https://doi.org/10.1016/j.envpol.2019.113679, 2020.

Han, C., Ding, S. M., Yao, L., Shen, Q. S., Zhu, C. G., Wang, Y., and Xu, D.: Dynamics of phosphorus-iron-sulfur at the sediment-water interface influenced by algae blooms decomposition, J. Hazard. Mater., 300, 329–337, https://doi.org/10.1016/j.jhazmat.2015.07.009, 2015.

Hansel, C. M., Lentini, C. J., Tang, Y. Z., Johnston, D. T., Wankel, S. D., and Jardine, P. M.: Dominance of sulfur-fueled iron oxide reduction in low-sulfate freshwater sediments, ISME J., 9, 2400–2412, https://doi.org/10.1038/ismej.2015.50, 2015.

Ho, J. C., Michalak, A. M., and Pahlevan, N.: Widespread global increase in intense lake phytoplankton blooms since the 1980s, Nature, 574, 667–670, https://doi.org/10.1038/s41586-019-1648-7, 2019.

Holmer, M. and Storkholm, P.: Sulphate reduction and sulphur cycling in lake sediments: a review, Freshwater Biol., 46, 431–451, https://doi.org/10.1046/j.1365-2427.2001.00687.x, 2001.

Hsieh, Y. P. and Shieh, Y. N.: Analysis of reduced inorganic sulfur by diffusion methods: improved apparatus and evaluation for sulfur isotopic studies, Chem. Geol., 137, 255–261, 1997.

Iwayama, A., Ogura, H., Hirama, Y., Chang, C. W., Hsieh, C. H., and Kagami, M.: Phytoplankton species abundance in Lake

Inba (Japan) from 1986 to 2016, Ecol. Res., 32, 783–783, https://doi.org/10.1007/s11284-017-1482-z, 2017.

Jorgensen, B. B., Findlay, A. J., and Pellerin, A.: The Biogeochemical sulfur cycle of Marine sediments, Front. Microbiol., 10, 849, https://doi.org/10.3389/fmicb.2019.00849, 2019.

Liu, Z. S., Zhang, Y., Han, F., Yan, P., Liu, B. Y., Zhou, Q. H., Min, F. L., He, F., and Wu, Z. B.: Investigation on the adsorption of phosphorus in all fractions from sediment by modified maifanite, Sci. Rep., 8, 15619, https://doi.org/10.1038/s41598-018-34144-w, 2018.

Mao, Z. G., Gu, X. H., Cao, Y., Luo, J. H., Zeng, Q. F., Chen, H. H., and Jeppesen, E.: How does fish functional diversity respond to environmental changes in two large shallow lakes?, Sci. Total Environ., 753, 142158, https://doi.org/10.1016/j.scitotenv.2020.142158, 2021.

Mort, H. P., Slomp, C. P., Gustafsson, B. G., and Andersen, T. J.: Phosphorus recycling and burial in Baltic sea sediments with contrasting redox conditions, Geochim. Cosmochim. Ac., 74, 1350–1362, https://doi.org/10.1016/j.gca.2009.11.016, 2010.

Melemdez-Pastor, I., Isenstein, E. M., Navarro-Pedreno, J., and Park, M. H.: Spatial variability and temporal dynamics of cyanobacteria blooms and water quality parameters in Missisquoi Bay (Lake Champlain), Water Supply, 19, 1500–1506, https://doi.org/10.2166/ws.2019.017, 2019.

Nakagawa, M., Ueno, Y., Hattori, S., Umemura, M., Yagi, A., Takai, K, Koba, K., Sasaki, Y., Makabe, A., and Yoshida, N.: Seasonal change in microbial sulfur cycling in monomictic Lake Fukami-ike, Japan, Limnol. Oceanogr., 57, 974–988, https://doi.org/10.4319/lo.2012.57.4.0974, 2012.

Ni, Z. K., Wang, S. R., Wu, Y., and Pu, J.: Response of phosphorus fractionation in lake sediments to anthropogenic activities in China, Sci. Total Environ., 699, 134242, https://doi.org/10.1016/j.scitotenv.2019.134242, 2020.

Pan, P., Guo, Z. R., Cai, Y., Liu, H. T., Wang, B., and Wu, J. Y.: High-resolution imaging of labile P&S in coastal sediment: Insight into the kinetics of P mobilization associated with sulfate reduction, Mar. Chem., 225, 103851, https://doi.org/10.1016/j.marchem.2020.103851, 2020.

Pester, M., Knorr, K. H., Friedrich, M. W., Wagner, M., and Loy, A.: Sulfate-reducing microorganisms in wetlands-fameless actors in carbon cycling and climate change, Front. Microbiol., 3, https://doi.org/10.3389/fmicb.2012.00072, 2012.

Phillips, E. J. P. and Lovley, D. R.: Determination of Fe(III) and Fe(II) in Oxalate Extracts of Sediment, Soil Sci. Soc. Am. J., 51, 938–941, 1987.

Roden, E. E.: Geochemical and microbiological controls on dissimilatory iron reduction, C.R. Geosci., 338, 456–467, https://doi.org/10.1016/j.crte.2006.04.009, 2006.

Ruban, V., Lopez-Sanchez, J.F., Pardo, P., Rauret, G., Muntau, H., and Quevauviller, P.: Harmonized protocol and certified reference material for the determination of extractable contents of phosphorus in freshwater sediments-A synthesis of recent works, Fresen. J. Anal. Chem., 370, 224–228, https://doi.org/10.1007/s002160100753, 2001.

Sela-Adler, M., Ronen, Z., Herut, B., Antler, G., Vigderovich, H., Eckert, W., and Sivan, O.: Co-existence of Methanogenesis and sulfate reduction with common substrates in sulfate-rich estuarine sediments, Front. Microbiol., 8, 766, https://doi.org/10.3389/fmicb.2017.00766, 2017.

Tabatabai, M.: A rapid method for determination of sulfate in water samples, Environmental, 7, 237–243, 1974.

Taylor, K. G. and Konhauser, K. O.: Iron in Earth surface systems: a major player in chemical and biological processes, Elements, 7, 83–87, https://doi.org/10.2113/gselements.7.2.83, 2011.

Thamdrup, B., Dalsgaard, T., Jensen, M. M., and Petersen, J.: Anammox and the marine N cycle, Geochim. Cosmochim. Ac., 68, A325, 2004.

Wu, S. J., Zhao, Y. P., Chen, Y. Y., Dong, X. M., Wang, M. Y., and Wang, G. X.: Sulfur cycling in freshwater sediments: A cryptic driving force of iron deposition and phosphorus mobilization, Sci. Total Environ., 657, 1294–1303, https://doi.org/10.1016/j.scitotenv.2018.12.161, 2019.

Xu, G. H., Sun, Z. H., Fang, W. Y., Liu, J. J., Xu, X. B., and Lv, C. X.: Release of phosphorus from sediments under wave-induced liquefaction, Water Res., 144, 503–511, https://doi.org/10.1016/j.watres.2018.07.038, 2018.

Yan, X. C., Xu, X. G., Wang, M. Y., Wang, G. X., Wu, S. J., Li, Z. C., Sun, H., Shi, A., and Yang, Y. H.: Climate warming and cyanobacteria blooms: Looks at their relationships from a new perspective, Water Res., 125, 449–457, https://doi.org/10.1016/j.watres.2017.09.008, 2017.

Yu, T., Zhang, Y., Wu, F. C., and Meng, W.: Six-Decade change in water chemistry of large freshwater lake Taihu, China, Environ. Sci. Technol., 47, 9093–9101, https://doi.org/10.1021/es401517h, 2013.

Zhang, S. Y., Zhao, Y. P., Zhou, C. Q., Duan, H. X., and Wang, G. X.: Dynamic sulfur-iron cycle promoted phosphorus mobilization in sediments driven by the algae decomposition, Ecotoxicology, 30, 1662–1671, https://doi.org/10.1007/s10646-020-02316-y, 2020.

Zhao, Y. P., Zhang, Z. Q., Wang, G. X., Li, X. J., Ma, J., Chen, S., Deng, H., and Annalisa, O. H.: High sulfide production induced by algae decomposition and its potential stimulation to phosphorus mobility in sediment, Sci, Total Environ., 650, 163–172, https://doi.org/10.1016/j.scitotenv.2018.09.010, 2019.

Zhao, Y. P., Wu, S. J., Yu, M. T., Zhang, Z. Q., Wang, X., Zhang, S. Y., and Wang, G. X.: Seasonal iron-sulfur interactions and the stimulated phosphorus mobilization in freshwater lake sediments, Sci. Total Environ., 768, 144336, https://doi.org/10.1016/j.scitotenv.2020.144336, 2021.

Zhou, C. Q., Peng, Y., Deng, Y., Yu, M. T., Chen, L., Zhang, L. Q., Xu, X. G., Zhao, F. J., Yan, Y., and Wang, G. X.: Increasing sulfate concentration and sedimentary decaying cyanobacteria co-affect organic carbon mineralization in eutrophic lakes sediments, Sci. Total Environ., 806, 151260, https://doi.org/10.1016/j.scitotenv.2021.151260, 2022.